Affinity Classification of Kinase Inhibitors by Mass Spectrometric Methods and Validation Using Standard IC50 Measurements

8 AUTHORS, INCLUDING:

David Touboul
Natural Product Chemistry Institute
118 PUBLICATIONS **2,009** CITATIONS

SEE PROFILE

Rishi Jain
Novartis Institutes for BioMedical Research
28 PUBLICATIONS **708** CITATIONS

SEE PROFILE

John A Tallarico
Novartis
51 PUBLICATIONS **2,446** CITATIONS

SEE PROFILE

Paul Ramage
Novartis
32 PUBLICATIONS **1,138** CITATIONS

SEE PROFILE

Article

Affinity Classification of Kinase Inhibitors by Mass Spectrometric Methods and Validation Using Standard IC Measurements

Matthias Conradin Jecklin, David Touboul, Rishi Jain, Estee Naggar
Toole, John Tallarico, Peter Drueckes, Paul Ramage, and Renato Zenobi

More About This Article

Additional resources and features associated with this article are available within the HTML version:

- Supporting Information
- Access to high resolution figures
- Links to articles and content related to this article
- Copyright permission to reproduce figures and/or text from this article

View the Full Text HTML

Affinity Classification of Kinase Inhibitors by Mass Spectrometric Methods and Validation Using Standard IC$_{50}$ Measurements

Matthias Conradin Jecklin,[†] David Touboul,[†] Rishi Jain,[‡] Estee Naggar Toole,[‡] John Tallarico,[‡] Peter Drueckes,[§] Paul Ramage,[§] and Renato Zenobi*,[†]

Department of Chemistry and Applied Biosciences, ETH Zürich, CH-8093 Zürich, Switzerland, Novartis Institutes for Biomedical Research, 250 Mass Avenue, Cambridge, Massachusettts 02139, and Novartis Institutes for Biomedical Research, Basel, Switzerland

Protein kinases have emerged as a major drug target in the last years. Since more than 500 kinases are encoded in the human genome, cross-reactivity of a majority of kinase inhibitors causes problems. Tools are required for a rapid classification of inhibitors according to their affinity for a certain target to refine the search for new, more specific lead compounds. Mass spectrometry (MS) is increasingly used in pharmaceutical research and drug discovery to investigate protein−ligand interactions and determination of binding affinities. We present a comparison of different existing nanoelectrospray-MS based methods to quantify binding affinities and qualitatively rank, by competitive experiments, the affinity of several clinical inhibitors. We also present a new competitive method which is derived from our previous work for quantitative assessment of binding strengths (Wortmann et al., *J. Mass Spectrom.* 2008, *43*(5), 600−608). The human kinases studied for this purpose were p38α (MAPK14) and LCK (lymphocyte specific kinase), and their interaction with 17 known small molecule kinase inhibitors was probed. Moreover, we present a new method to differentiate type I from type II inhibitors (Liu, Y.; Gray, N. S. *Nat. Chem. Biol.* 2006, *2*(7), 358−364) based on a kinetic experiment with direct MS read-out of the noncovalent complex between the human kinase and the inhibitor. This method was successfully applied to p38α binding to BIRB796, as well as to a BIRB796 analogue. Quantitative determination of the binding strength is also described. The results of our competitive experiments for the affinity classification of different inhibitors, as well as the results for the kinetic study, are in good agreement with IC$_{50}$ measurements and data found in the literature.

More than 500 kinases (enzymes involved in phosphorylation reactions) are encoded in the human genome and play key roles in all aspects of cellular physiology.[1] Abnormal kinase activity is a cause or consequence of diseases including inflammation, cancer, and cellular transformations in leukemia.[2] Therefore, it is not surprising that an estimated 25% of all pharmaceutical drug targets are protein kinases.[3] Several kinase inhibitors have already been approved for clinical use, and many others are undergoing human clinical trials for the treatment of different diseases.[3] Because of the conservation of the ATP binding site[1] there is great potential for cross-reactivity of such compounds,[4] and they must be tested experimentally against many kinases to determine their specificity.

Different approaches have been proposed to assess the binding specificity of kinase inhibitors binding to the ATP site of kinases. In the work of Davies et al.[5] and Bain et al.[4] a list of test compounds was screened against a panel of several kinase targets and their affinity determined by a radioactivity assay (competition and displacement of [$\gamma-33$]ATP by the test compound). The drawback of this method is the cost of the radio-labeled compounds and the need for a radioactive laboratory operated by safety and waste-handling trained personnel. Because of these concerns, homogeneous (Lantha, Invitrogen) and heterogeneous (Caliper Life Sciences) fluorescence based methods have largely gained popularity as primary screening methods for the discovery of kinase inhibitors. In spite of their wide usage, the above techniques are still vulnerable to detection of false positives because of the prevalence of promiscuous inhibition through small molecule aggregation.[6−8] Following high throughput screening (HTS), where multiple hits are generated and selected for follow-up, there is a strong need for a robust binding assay that does not rely on biochemical inhibition but rather allows the user to read out

* To whom correspondence should be addressed. E-mail: zenobi@org.chem.ethz.ch.
† ETH Zürich.
‡ Novartis Institutes for Biomedical Research, Cambridge.
§ Novartis Institutes for Biomedical Research, Basel.

(1) Manning, G.; Whyte, D. B.; Martinez, R.; Hunter, T.; Sudarsanam, S. *Science* **2002**, *298*, 1912–1934.
(2) Hunter, T. In *Harvey Lectures, Series 94, 1998−1999*; Wiley: New York, 2000; Vol. 94, p 81.
(3) Cohen, P. *Nat. Rev. Drug Discovery* **2002**, *1*, 309–315.
(4) Bain, J.; McLauchlan, H.; Elliott, M.; Cohen, P. *Biochem. J.* **2003**, *371*, 199–204.
(5) Davies, S. P.; Reddy, H.; Caivano, M.; Cohen, P. *Biochem. J.* **2000**, *351*, 95–105.
(6) McGovern, S. L.; Helfand, B. T.; Feng, B.; Shoichet, B. K. *J. Med. Chem.* **2003**, *46*, 4265–4272.
(7) McGovern, S. L.; Shoichet, B. K. *J. Med. Chem.* **2003**, *46*, 1478–1483.
(8) Seidler, J.; McGovern, S. L.; Doman, T. N.; Shoichet, B. K. *J. Med. Chem.* **2003**, *46*, 4477–4486.

affinity, binding mode, and stoichiometry all on unlabeled protein and small molecule. Isothermal titration calorimetry (ITC) is one technique that has gained popularity over the years which achieves this. Unfortunately, the high protein quantity required in addition to low throughput hampers its usage for screening multiple compounds/proteins. In a novel assay described by Fabian et al.[9] kinase domains are expressed as fusions to a T7 bacteriophage. The test inhibitors in solution compete with immobilized "bait" compounds for binding to the ATP site of each kinase. The amount of phage bound to the immobilized ligand is then quantified to determine the inhibitor's affinity to the target kinase domain. The issues here are the preservation of conformation of the kinase domain in fusion to the bacteriophage and the indirect quantification using quantitative polymerase chain reaction (PCR) measurements. In 2007, a new proteomics method for quantifying on- and off-target effects of kinase inhibitors in vivo was presented by Bantscheff et al.[10] Their method is based on "kinobeads" which display multiple kinase inhibitors and preferentially bind kinases (and other purine-binding proteins) from cell lysates. Using an isobaric tag for relative and absolute quantitation (iTRAQ) to monitor binding of specific proteins to the beads as concentrations of a free kinase inhibitor are increased, they were able to determine affinity binding constants for hundreds of kinases from multiple cell lines and tissues.

As described in the review of Hofstadler et al.,[11] electrospray ionization mass spectrometry (ESI-MS) is gaining more and more attention for applications in drug discovery. In principle, non-isobaric species can universally be detected and quantified by MS. In the instance of ligand-protein interactions, detection of ions belonging to bound versus unbound species allow a K_D calculation. Furthermore, if the formed protein–ligand complex can be directly detected, one can easily determine the stoichiometry of binding as the mass change upon complexation should be integer increments of the MW of bound small molecule. Finally, if a known inhibitor is available, one can displace this inhibitor in the presence of the test compound and conclude whether the mode of binding is competitive or noncompetitive. Various methods have emerged for inhibitor screening from large compound libraries to select a lead group in the early stages of target based drug discovery.[12,13] Moreover, much effort is put into quantifying the strength of noncovalent interactions between protein-small molecule, protein–protein, DNA-small molecule, and DNA–protein systems.[14−16]

Most small molecule kinase inhibitors developed so far bind in a competitive way as they target the ATP binding site in an active protein conformation. This class of inhibitors is referred to as type I inhibitors.[17] Recently, however, a new class of kinase inhibitors has been identified using structure−activity relationship (SAR)-guided approaches combined with NMR or X-ray. By binding to an inactive conformation of the kinase, these so-called type II inhibitors prevent activation.[18] These small molecules occupy the ATP binding site but also show characteristic hydrogen bonding and hydrophobic interactions with the highly conserved Asp-Phe-Gly (DFG) motif.[17] From NMR studies it is known that type I inhibitors can bind to the active protein ("DFG-in"), as well as to the inactive protein conformation ("DFG-out").[19] In the "DFG-in" conformation the Phe residue is buried in a hydrophobic pocket in the groove between the two lobes of the kinase. On the contrary, type II inhibitors only bind to the "DFG-out" conformation, where the DFG loop has moved to a new position revealing a large hydrophobic pocket. Because only kinases able to adopt this "DFG-out" conformation can interact with a type II inhibitor and this hydrophobic pocket, selectivity is given by this selection of conformational space of the kinase. Several distinct type II kinase inhibitors have been described so far,[17] for example, imatinib binding Abelson kinase,[20] and BIRB796 binding p38α,[21] with the latter showing surprisingly slow binding kinetics.[19,21,22]

The aim of this work was to investigate the feasibility of nanoESI-MS to classify known type I and type II inhibitors according to their affinity to two protein kinase targets. The automated chip-based nanoelectrospray device (NanoMate Model 100, Advion Bioscience, Ithaca, NY) used for our work is common for proteomic studies because of its fast and reproducible performance, as well as low sample consumption (a few pmol of protein per measurement).[23,24] Table 1 shows the small molecule inhibitors tested for the two protein targets examined here. The first protein investigated was p38α (MAPK14), a member of the Mitogen-activated protein kinase (MAPK) cascade signaling pathway.[25] The second protein was

(9) Fabian, M. A.; Biggs, W. H.; Treiber, D. K.; Atteridge, C. E.; Azimioara, M. D.; Benedetti, M. G.; Carter, T. A.; Ciceri, P.; Edeen, P. T.; Floyd, M.; Ford, J. M.; Galvin, M.; Gerlach, J. L.; Grotzfeld, R. M.; Herrgard, S.; Insko, D. E.; Insko, M. A.; Lai, A. G.; Lelias, J. M.; Mehta, S. A.; Milanov, Z. V.; Velasco, A. M.; Wodicka, L. M.; Patel, H. K.; Zarrinkar, P. P.; Lockhart, D. J. *Nat. Biotechnol.* **2005**, *23*, 329–336.

(10) Bantscheff, M.; Eberhard, D.; Abraham, Y.; Bastuck, S.; Boesche, M.; Hobson, S.; Mathieson, T.; Perrin, J.; Raida, M.; Rau, C.; Reader, V.; Sweetman, G.; Bauer, A.; Bouwmeester, T.; Hopf, C.; Kruse, U.; Neubauer, G.; Ramsden, N.; Rick, J.; Kuster, B.; Drewes, G. *Nat. Biotechnol.* **2007**, *25*, 1035–1044.

(11) Hofstadler, S. A.; Sannes-Lowery, K. A. *Nat. Rev. Drug Discovery* **2006**, *5*, 585–595.

(12) Deng, G. J.; Sanyal, G. *J. Pharm. Biomed. Anal.* **2006**, *40*, 528–538.

(13) Greis, K. D. *Mass Spectrom. Rev.* **2007**, *26*, 324–339.

(14) Daniel, J. M.; Friess, S. D.; Rajagopalan, S.; Wendt, S.; Zenobi, R. *Int. J. Mass Spectrom.* **2002**, *216*, 1–27.

(15) Tjernberg, A.; Carno, S.; Oliv, F.; Benkestock, K.; Edlund, P. O.; Griffiths, W. J.; Hallen, D. *Anal. Chem.* **2004**, *76*, 4325–4331.

(16) Wortmann, A.; Jecklin, M. C.; Touboul, D.; Badertscher, M.; Zenobi, R. *J. Mass Spectrom.* **2007**, *43*, 600–608.

(17) Liu, Y.; Gray, N. S. *Nat. Chem. Biol.* **2006**, *2*, 358–364.

(18) Mol, C. D.; Fabbro, D.; Hosfield, D. J. *Curr. Opin. Drug Discovery Dev.* **2004**, *7*, 639–648.

(19) Vogtherr, M.; Saxena, K.; Hoelder, S.; Grimme, S.; Betz, M.; Schieborr, U.; Pescatore, B.; Robin, M.; Delarbre, L.; Langer, T.; Wendt, K. U.; Schwalbe, H. *Angew. Chem., Int. Ed.* **2006**, *45*, 993–997.

(20) Schindler, T.; Bornmann, W.; Pellicena, P.; Miller, W. T.; Clarkson, B.; Kuriyan, J. *Science* **2000**, *289*, 1938–1942.

(21) Pargellis, C.; Tong, L.; Churchill, L.; Cirillo, P. F.; Gilmore, T.; Graham, A. G.; Grob, P. M.; Hickey, E. R.; Moss, N.; Pav, S.; Regan, J. *Nat. Struct. Biol.* **2002**, *9*, 268–272.

(22) Zaman, G. J. R.; van der Lee, M. M. C.; Kok, J. J.; Nelissen, R. L. H.; Loomans, E. *Assay Drug Dev. Technol.* **2006**, *4*, 411–420.

(23) Zhang, S.; Van Pelt, C. K. *Expert Rev. Proteomics* **2004**, *1*, 449–468.

(24) Zhang, S.; Van Pelt, C. K.; Wilson, D. B. *Anal. Chem.* **2003**, *75*, 3010–3018.

(25) Kumar, S.; Boehm, J.; Lee, J. C. *Nat. Rev. Drug Discovery* **2003**, *2*, 717–726.

Table 1. Numbers, Names, Structures, And Chemical Properties of the Small Molecule Inhibitors Investigated[a]
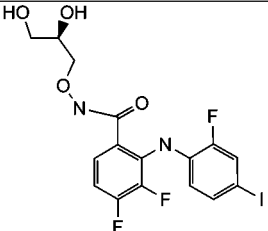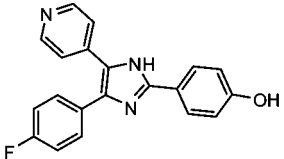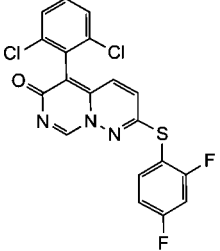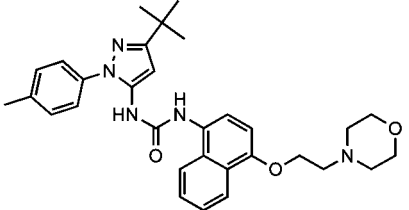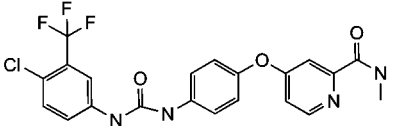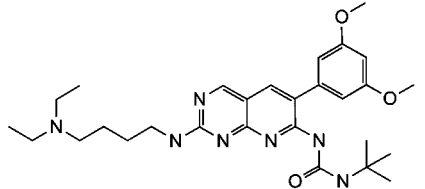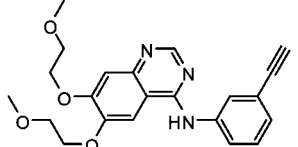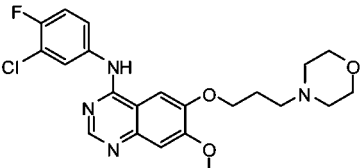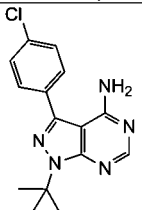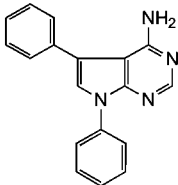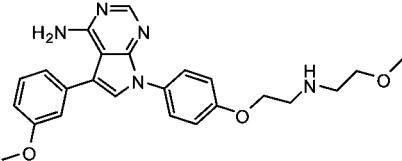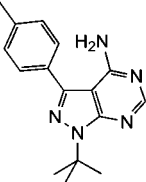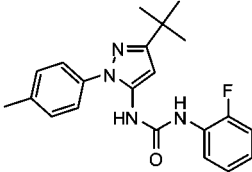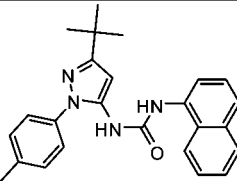
Number	Name or class	Structure	Molecular Formula	Exact mass
1	PD0325901		$C_{16}H_{14}F_3IN_2O_4$	482.00
2	SB202190		$C_{20}H_{14}FN_3O$	331.11
3	VX-745		$C_{19}H_9Cl_2F_2N_3OS$	434.98
4	BIRB796		$C_{31}H_{37}N_5O_3$	527.29
5	Bay43-9006		$C_{21}H_{16}ClF_3N_4O_3$	464.09
6	PD-173074		$C_{28}H_{41}N_7O_3$	523.33
7	Erlotinib Tarceva		$C_{22}H_{23}N_3O_4$	393.17
8	Gefinitib Iressa		$C_{22}H_{24}ClFN_4O_3$	446.15
9	PP2		$C_{15}H_{16}ClN_5$	301.11

Table 1. Continued

Number	Name or class	Structure	Molecular Formula	Exact mass
10	CGP062464		$C_{18}H_{14}N_4$	286.12
11	CGP076030		$C_{24}H_{27}N_5O_3$	433.21
12	PP1		$C_{16}H_{19}N_5$	281.16
13	Pyrazole-urea	not reported		
14	Pyrazole-urea	not reported		
15	Pyrazole-urea	not reported		
16	Pyrazole-urea		$C_{21}H_{23}FN_4O$	366.19
17	Pyrazole-urea		$C_{25}H_{26}N_4O$	398.21

[a] For the BIRB796 analogues **13**, **14**, **15** no information is given because of patent reasons.

the Src-family lymphocyte-specific protein tyrosine kinase LCK, a protein involved in T-cell activation and signal transduction.[26]

Three different quantitative methods were applied to get a dissociation constant (K_D) of a compound. Two competitive methods were then applied to get a relative affinity order of the rest of the examined compounds (see experimental section for more details). The goal of this work was on one hand to apply MS-based titration methods on one of the inhibitors, to rapidly screen it for its "affinity class" (i.e., 1−10 nM, 10−100 nM, 0.1−1 μM, 1−10 μM range) and to afterwards use it as reference to determine an affinity order against other inhibitors binding to the same protein kinase target using competition experiments. The outcomes of these measurements are compared with IC_{50} measurements (Lantha for the LCK binding assay and Caliper for the p38 binding assay), as well as other techniques reported in literature.

(26) Zhu, X. T.; Kim, J. L.; Newcomb, J. R.; Rose, P. E.; Stover, D. R.; Toledo, L. M.; Zhao, H. L.; Morgenstern, K. A. *Struct. Folding Des.* **1999**, *7*, 651–661.

EXPERIMENTAL SECTION

Instrumentation. Mass spectrometric analysis was performed with a hybrid quadrupole time-of-flight mass spectrometer (Q-Tof Ultima; Waters/Micromass Ltd., Manchester, U.K.) equipped with a chip-based nanoESI robot (NanoMate Model 100, Advion Bioscience, Ithaca, NY, U.S.A.). The voltage applied was 1.6−1.7 kV using a gentle backing pressure of 4−6 bar for all nanoESI-MS measurements, resulting in an estimated flow rate of a few 100 nL/min. The mass spectrometer was controlled via the MassLynx version 4.0 software. All measurements were performed in the positive ion mode. The source temperature was kept at 50 °C. After atmospheric pressure sampling of the ions, they were transmitted through the so-called ion tunnels. The pressure in this region was optimized for each protein using a throttle valve (Speedivalve, Edwards, West Sussex, U.K.). After this stage, the ion beam passed a quadrupole operated in RF-only mode and then a hexapole collision cell filled with argon (Purity 5.0, PanGas). Calibration of the instrument from m/z 200−6000 was performed using the cesium iodide (CsI) clusters generated by spraying a

solution of CsI in water/2-propanol (1/1, v/v) at a concentration of 2 μg/μL.

The optimal instrumental conditions to observe p38α and its noncovalent inhibitor complexes were cone voltage, 45 V; RF1 lens, 200 V; collision energy setting, 20 V. Moreover, the pressure in the first pumping stage was increased to 3.9−4.1 mbar using the valve. Instrumental conditions for the observation of LCK and its complexes were cone voltage, 50 V; RF1 lens, 100 V; collision energy setting, 17 V. The pressure in the first pumping stage was kept at 1.9−2.0 mbar, which is the standard operating pressure of the instrument. For the CID experiments only the hexapole voltage, which determines the collision energy, was varied.

Materials. All solvents and buffer components were purchased from Sigma-Aldrich (Buchs, Switzerland). MAPK14 p38α (MW = 42.3 kDa), LCK (MW = 30.6 kDa), as well as small molecule inhibitors, (see Table 1) were provided by Novartis Institute of Biomedical Research. Stock solutions at 5−20 mM of each compound were prepared in methanol and stored in the dark at 4 °C overnight. The compound solutions were further diluted to the working concentration described for the individual methods in the nondenaturing buffer. For nondenaturing conditions we used a 20 mM ammonium bicarbonate buffer at pH 7.2 (pH was adjusted with dry ice) and a mixture of water/methanol/acetic acid (50/50/1, v/v/v) for denaturing conditions. Prior to mass spectrometric analysis, both protein samples were desalted using Micro Bio-Spin 6 columns (BioRad, Hercules, CA, USA) with a 6 kDa cutoff equilibrated with the nondenaturing buffer.

For mass spectrometric analysis of p38α and LCK, a 5 μM protein solution was used, diluted from a 1 mM protein stock solution. The protein concentrations were determined using RP-HPLC (precalibrated using an interleukin-6 standard, denaturing conditions, detection at 210 nm measuring peptide bond absorption and thereby minimizing protein−protein variation). For the competition experiments performed for this work, the exact protein concentration is not required. For the performed titration measurements and kinetic experiments, however, a more precise protein concentration had to be determined. The determination of the real concentration of p38α is described later, in the section "Kinetic Method".

Mass Spectrometry Based Methods. *Noncovalent Titration Method.* The first titration method for K_D determination was adapted from Daniel et al.[27] It uses a plot of intensity ratio of complexed/free protein versus the total inhibitor concentration. The titration curve obtained is then fitted using the equation described by Daniel et al. with the Origin 7.5 software (OriginLab Corporation, Northampton, MA U.S.A.). The three other methods used to determine an affinity order of the small molecule inhibitors are described in the following.

Noncovalent Complex Competition Method. The first competition method is based on monitoring the noncovalent protein−ligand complex signals of two different inhibitors competing for binding to protein. The signal of the protein complexed with the tighter binder will appear at higher intensity compared to the protein complexed with the weaker binder. By increasing the concentration of the weaker binder, the tighter binder can be successively displaced, indicated by a gradual change of the corresponding signal intensities. Under the assumptions that (i) the small molecule inhibitor does not alter the ionization efficiency of the protein and (ii) free protein and protein complexes have the same transmission through the mass spectrometer, a relative binding order can be estimated. Similar techniques have already been described.[15,28]

Titration Method in the Low Mass Range. A novel technique has been introduced only recently by our laboratory for the quantitative K_D determination.[16] This methodology relies only on the determination of signal intensity ratios for free ligands in the low mass region and allows the K_D of very high affinity protein−ligand systems to be calculated.

Ligand Depletion Method. This method was applied in this work for the first time to rank the inhibitors by affinity. With the mass spectrometer tuned for small molecule detection (low CID energy, low RF voltages for a "soft" ion transmission and as little destruction of noncovalent interactions as possible), the signal of two inhibitors in an equimolar mixture (e.g., 3.3 μM) in nondenaturing buffer is monitored. The intensity ratio of the two compounds reflects their ionization efficiency in the nanoelectrospray process (reference spectrum). Then, protein is added to this mixture in increasing amounts (e.g., 3.3, 6.7, and 10 μM). The ratio of the inhibitor signals will change according to their affinity for the added protein target. With one reference spectrum and 2−3 measurements with increasing amounts of added protein, the relative binding affinity of two inhibitors is easily determined. It is evident that this method is limited to inhibitors competing for the same binding pocket. An advantage of this technique is that no assumptions about ionization efficiency and response factors of bound and unbound protein species are necessary.[29]

Kinetic Method. This method is based on determining the observed kinetic constant for the binding event of the small molecule inhibitor to the protein. The equation for the binding of a ligand L to p38α can be described as

$$\text{p38}\alpha + \text{L} \underset{k_{\text{off}}}{\overset{k_{\text{on}}}{\rightleftharpoons}} (\text{p38}\alpha \cdot \text{L}) \tag{1}$$
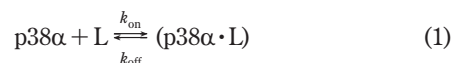
The kinetic constants k_{on} and k_{off} stand for the forward and backward reaction, respectively. Under equilibrium conditions, their relationship is described by the following equation (definition of dissociation constant):

$$K_D = \frac{[\text{p38}\alpha][\text{L}]}{[\text{p38}\alpha \cdot \text{L}]} = \frac{k_{\text{off}}}{k_{\text{on}}} \tag{2}$$

where [p38α], [L], and [p38α·L] designate the free protein, ligand, and complex concentrations.

As previously shown by Weiland et al.,[30] a pseudofirst order approximation can be used when $[\text{L}]_0 > 10 \times [\text{p38}\alpha]_0$. When

(27) Daniel, J. M.; McCombie, G.; Wendt, S.; Zenobi, R. *J. Am. Soc. Mass Spectrom.* **2003**, *14*, 442−448.

(28) Nesatyy, V. J. *Int. J. Mass Spectrom.* **2002**, *221*, 147−161.
(29) Gabelica, V.; Galic, N.; Rosu, F.; Houssier, C.; De Pauw, E. *J. Mass Spectrom.* **2003**, *38*, 491−501.
(30) Weiland, G. A.; Molinoff, P. B. *Life Sci.* **1981**, *29*, 313−330.

p38α is incubated with a slow binding compound the decreasing p38α signal can be monitored with time. The measurement of such slopes of pseudo-first order plots over a range of ligand concentrations give access to k_{on} and k_{off}:

$$k_{obs} = k_{on}[L]_0 + k_{off} \qquad (3)$$

where k_{obs} is the "observed kinetic constant". The curve fitting and kinetic constant determination for this model was performed using the Origin 7.5 software (OriginLab Corporation, Northampton, MA, U.S.A.). This method has the advantage that it does not require the exact protein concentration, as needed, for example, for the titration method and K_D determination.[27] The scan time for the full m/z range was 0.2 s; the signal was accumulated over 2 s giving a time resolution of 2 s for the kinetic method. The concentrations used for **4** were 10, 15, 20, and 25 μM and 10, 12.5, 15, and 17.5 μM for **17**. The time needed to obtain one data point depends on the k_{on} rate and varies considerably, for example, from less than 2 min (25 μM) to around 30 min (10 μM) for compound **4**. A data set of four points was used for further evaluation and fitting of the kinetic rate constants and K_D determination.

IC50 Assays. For p38α, the IC$_{50}$ measurements were performed using the Caliper protein kinase profiling system (Caliper Life Sciences, Hopkinton, MA, U.S.A.) a widely used mobility shift microfluidic assay technology. The data readout is the shift in mobility of non-phosphorylated peptide substrate and phosphorylated product when separated on a chip by electrophoresis and detected via LED induced fluorescence. Product and substrate are directly measured using Caliper's technology and no radioactive isotopes or high affinity, specific antibodies are required. The assay was run for 1 h at 30 °C on a liquid handling robot with incubator. The final assay conditions were 50 mM HEPES pH 7.5, 1 mM DTT, 0.02% Tween20, 0.02% BSA, 8 mM MgCl$_2$, 2 μM peptide substrate, 300 μM ATP, and 5.4 nM p38α. After incubation, the reactions were terminated by addition of 16 μL of stop solution (100 mM HEPES, 5% DMSO, 10 mM EDTA, 0.015% Brij35). Subsequently, plates with terminated kinase reactions are transferred to a LC3000 Caliper workstation. In the microfluidic system of the instrument, unphosphorylated substrate and phosphorylated product are separated because of their different net charges by a combination of flow and electric field. Both substrate and product were quantified by measuring the laser-induced fluorescence intensities of the peptide's fluorescein labels and calculating the turnover. The dose-dependent influence of the compound on kinase activity is calculated and expressed as IC$_{50}$.

LCK was measured using the HTRF based Lanthascreen assay (Invitrogen Corporation, Carlsbad, CA, U.S.A.). The assay was run at room temperature on a liquid handling robot. To the assay plates containing 50 nL compound or control solutions, 4.5 μL of solution A (50 mM Tris-HCl pH 7.4, 2.0 mM DTT, 0.05% Tween20, 0.02 mM Na$_3$VO$_4$) including a generic concentration of 2.0 μM ATP was added per well, followed by 4.5 μL of solution B (0.5% BSA) including a generic concentration of 50 nM poly(EAY) to give 9.05 μL of a reaction volume with final concentrations of 2.0 μM ATP,
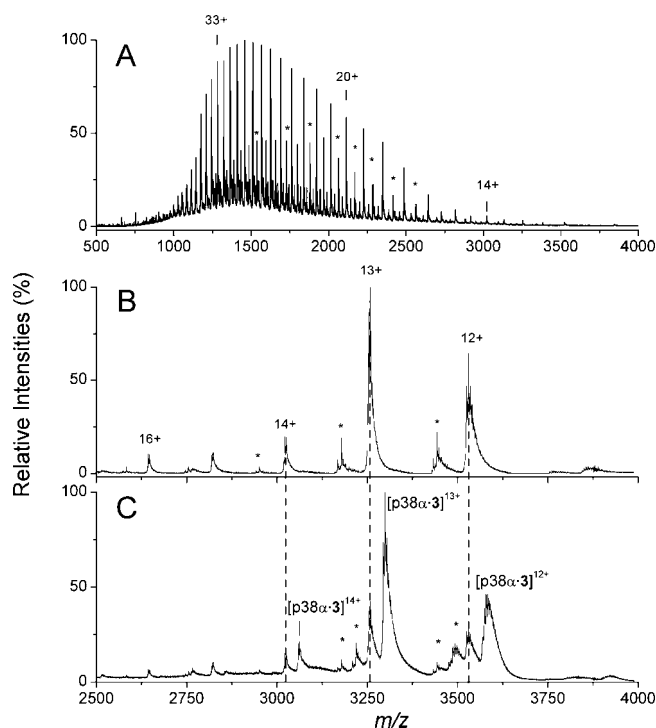

Figure 1. NanoESI mass spectra of p38α in (A) denaturing (water/ methanol/acetic acid, 50/50/1 (v/v/v)) and (B) nondenaturing (20 mM ammonium bicarbonate buffer at pH 7.2) conditions. * indicates a different isoform of p38α. (C) shows the spectrum of 5 μM p38α incubated with 20 μM of **3**. The dashed lines indicate the position of the free protein signals on the m/z scale and were added to guide the eye.

50 nM poly(EAY), 25 mM Tris-HCl pH 7.4, 1.0 mM DTT, 0.025% Tween20, 0.01 mM Na$_3$VO$_4$, 0.025%BSA, as well as specific concentration of the respective enzyme and individual concentrations of divalent cations. After 1 h of incubation, the kinase reactions have been stopped by the addition of 4.5 μL of stop solution D (48 mM EDTA, 0.08% CH$_3$COONa, 0.04% NP-40) immediately followed by 4.5 μL of solution A including the Tb-labeled P-20 antibody to detect phosphorylated poly(EAY) by time-resolved fluorescence resonance energy transfer (TR-FRET). After an incubation time of 45 min in the dark, the plates were transferred into a fluorescence reader for counting. The effect of compound on the enzymatic activity was obtained from the linear progress curves and determined from one reading (end point measurement).

RESULTS

p38α. The specificity of compound binding was first tested. Figure 1 shows mass spectra of p38α in denatured (A), and nondenatured form (B), and after incubation with compound **3** (C). For the first specificity test, denatured p38α (2 μM) was incubated with an excess of the tightly binding ligand **3** (10 μM). No binding was observed, indicating that all protein activity has been lost (data not shown). In addition, we performed a negative control experiment, mixing p38α under nondenaturing conditions with compound **13** at >10 fold excess. Again, no noncovalent complex was detected. **13** lacks the *t*-butyl group on the pyrrole ring, which is crucial for a
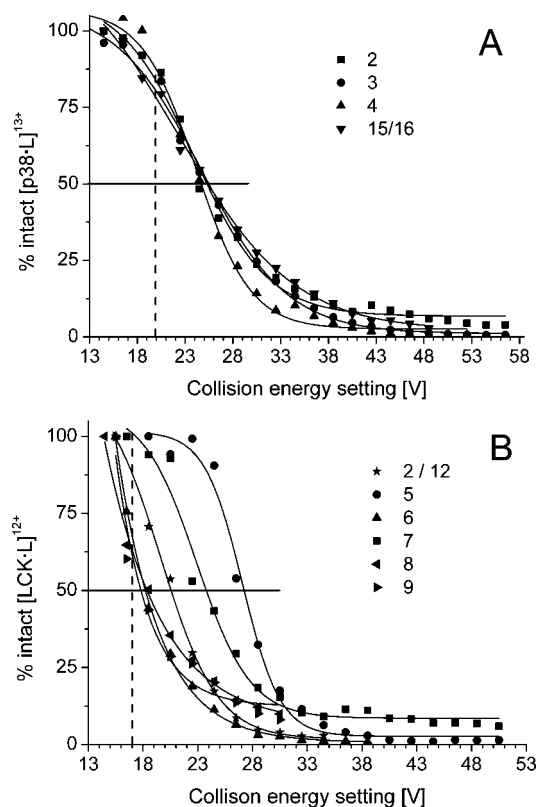
Figure 2. (A) Collision Induced Dissociation experiments of different noncovalent complexes between p38α and ligands. The percentage of intact complex, $100 \times I_{(P \cdot L)}/(I_{(P \cdot L)}+I_P)$ vs collision energy is plotted. The $[p38\alpha \cdot L]^{13+}$ ions all show the same behavior: 50% dissociation is achieved at a parameter setting of 25 V. (B) CID experiments of LCK with inhibitors show different stabilities in the gas phase. While compounds **2**, **6**, **8**, **9**, and **12** are almost completely dissociated at a collision energy setting of 25 V, the $[LCK \cdot 7]^{12+}$ complex is approximatively 50% dissociated and $[LCK \cdot 5]^{12+}$ is still >90% intact.

specific interaction[31] and, not surprisingly, showed very low affinity in a p38-ELISA assay (>10 μM, data not shown). In nondenaturing buffer, for the same concentration ratio, a noncovalent complex was observed for **3** with a 1:1 stoichiometry (Figure 1C). Identical tests were conducted for all the compounds, proving the specificity of the noncovalent binding observed with MS.

In a next step, collision induced dissociation (CID) experiments were performed for all noncovalent complexes of p38α (Figure 2A). These experiments are important because information can be gained on the stability of noncovalent complexes in the gas phase and their dissociation rate during the transmission through the mass spectrometer. We found that all noncovalent complexes have very similar gas phase stability, independent of their binding type in solution.[17] At a collision energy setting of around 25 V, 50% of all noncovalent complexes are dissociated. In the following experiments we choose a setting of 20 V where >70% of the noncovalent complexes are still intact. This setting is a good compromise between desolvation of the protein ions and some dissociation of the noncovalent complexes. Lower settings lead to very broad
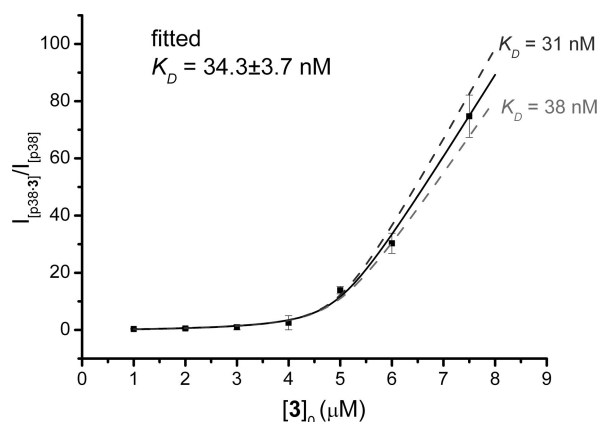
(31) Regan, J.; Pargellis, C. A.; Cirillo, P. F.; Gilmore, T.; Hickey, E. R.; Peet, G. W.; Proto, A.; Swinamer, A.; Moss, N. *Bioorg. Med. Chem. Lett.* **2003**, *13*, 3101–3104.

Figure 3. Titration curve obtained for p38α titrated with compound **3**. The titration experiment was repeated 3 times to determine the experimental error, and data was fitted as described by Daniel et al.[27] The determined K_D value is 34.3 ± 3.7 nM.

peaks, making it impossible to distinguish between free and complexed protein signals.

The affinity of compound **3** binding to p38α was determined using the titration method (see Experimental Section) and a K_D of 34.3 ± 3.7 nM was found (see Figure 3). Using the method described by Wortmann et al.,[16] the K_D of **3** binding to p38α was determined to be 4.7 nM.

Noncovalent Complex Competition Method. To classify the inhibitors by affinity for p38α, we applied the noncovalent complex competition method (see Experimental Section, Methods). Figure 4 shows representative mass spectra of the competitive experiment using ligand **5** and **16**. The mass spectrum of 5 μM p38α sprayed under nondenaturing conditions is shown in Figure 4A. The mass range *m/z* 3250−3375 is shown, where charge state 13+ of p38α is predominant. The large width of the signal observed for the free protein signal (Figure 4A) is not a problem of instrument resolution but is due to a partial acetylation on the protein (marked by an asterisk) and adduct formation with water and buffer components. Five μM of p38α were incubated with 10 μM of **16** as shown in Figure 4B. The noncovalent complexes of p38α with **5** or **16** also show this "decoration" of the signal, which makes differentiation difficult (Figure 4C, D). An increased concentration of **5** compared to **16** is needed (Figure 4E) to displace **16** from the binding pocket, indicated by the higher intensity of the $[p38\alpha \cdot 5]^{13+}$ compared to the $[p38\alpha \cdot 16]^{13+}$ complex. This information can be used to assign a higher affinity of compound **16** than **5** to the protein target p38α. This method was applied to all the compounds in a pairwise manner, and their relative affinity could be determined two by two. The final affinity order obtained by this method was **4** > **3** > **2** > **17** > **6** > **16** > **5** > **15** > **14** (≫**7, 8, 9, 10, 11, 12, 13**) where compounds **7−13** showed no or very weak binding to p38α (K_D >10 μM). The time required for each pairwise measurement is 10−15 min, that is, the whole set of data for one protein could be obtained within 8 h of measurement. The sample consumption per data point for these experiments was 25 pmol (5 μL of a 5 μM protein solution) of protein and 50−250 pmol (5 μL of a 10−50 μM inhibitor solution). Three or four data points were collected for assigning the relative binding affinity of two inhibitors.
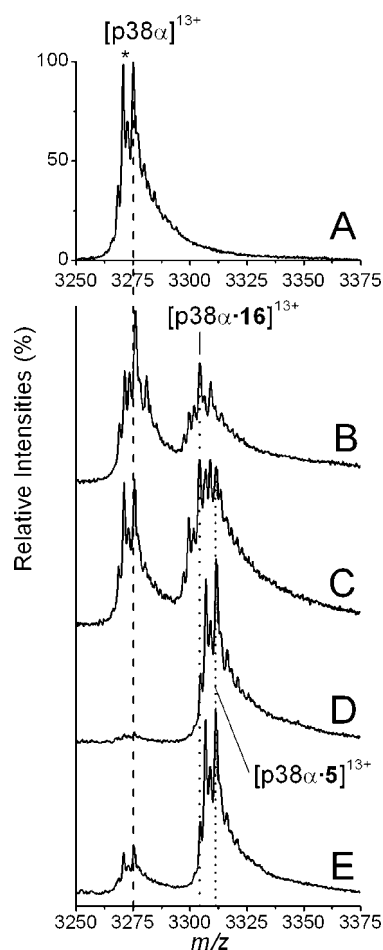
Figure 4. (A) NanoESI mass spectra of 5 μM p38α (in 20 mM ammonium bicarbonate buffer at pH 7.2). The signal for the free protein is quite broad, resulting from an acetylation present on the protein and different nonspecific adducts formed by buffer ions. (B) The noncovalent complex of p38α (5 μM) with compound **16** (10 μM) alone and (E) the complexes of p38α (5 μM) with **5** (10 μM) alone for charge state 13+. (C, D) A competition experiment: (C) p38α (5 μM) incubated with **5** at 20 μM and **16** at 10 μM, and (D) p38α (5 μM) in the presence of **5** at 50 μM and **16** at 10 μM. The concentration of **5** has to be increased by a factor of 5 to displace the tighter binder **16**. The dashed and dotted lines indicate the positions of acetylated protein (highest peak) and the corresponding (p38α·L) signals on the m/z scale, respectively.

Ligand Depletion Method. This method is based on monitoring the small molecule inhibitors directly in the lower m/z range as they are fading with increasing amounts of protein added to the sample solution. As described elsewhere,[16] this method has some clear advantages compared to the noncovalent complex competition method or studies of noncovalent interactions in the higher m/z range in general. Specifically, the benefits are better sensitivity and better resolution for small molecule detection in the lower mass range.

Figure 5 shows representative mass spectra of the ligand depletion method applied to compounds **3** and **16** binding to p38α. A representative mass spectrum of the inhibitors in the absence of the protein is shown in Figure 5A (reference spectrum), where **3** and **16** are sprayed at equimolar concentrations (3.3 μM) in nondenaturing buffer. The intensity ratio of compounds **3**/**16** is approximatively 4:1, from which the relative ionization efficiency can be directly determined. Figure
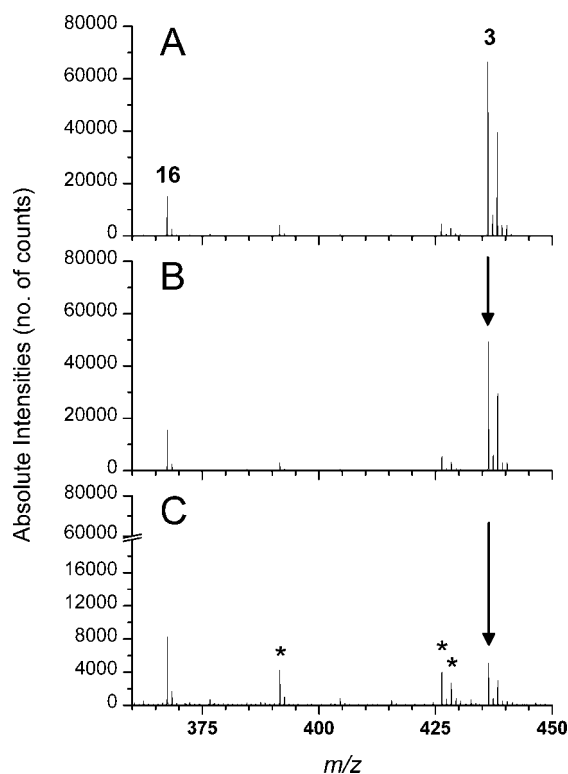

Figure 5. NanoESI mass spectra (accumulation of 300 scans each) of two compounds binding to p38α in competition for the binding site illustrating the ligand depletion method. (A) Reference mass spectrum of the two compounds alone (**3** and **16** at 3.3 μM), (B, C) **3** and **16** (each at 3.3 μM) in the presence of p38α at 6.6 μM and 10 μM, respectively. With increasing protein concentration, the relative signal ratio of the two inhibitors **3**/**16** changes from approximatively 4:1 (A), to 3:1 (B), and inverses to 1:2 (C). This implies that the binding affinity of **3** is higher than of **16** for the p38α protein target. (*) indicates impurities since almost all free ligand is bound to the protein (at an excess of protein); chemical noise is detected in the low m/z range.

5B shows the two compounds still at 3.3 μM but in the presence of 6.7 μM p38α. The relative intensity ratio of compounds **3**:**16** has decreased somewhat, to approximately 3:1. If the protein concentration is further increased to 10 μM this relative intensity ratio of compounds **3**/**16** is reversed, to around 1:2. This indicates that compound **3** is the tighter binder compared to **16**. In the same manner these experiments were extended to rank all inhibitors using this method, giving a final affinity order of (**4**$\approx$) **3** > **2** > **17** > **16** > **5** > (**6**$\approx$**15**) ($\gg$ **7, 8, 9, 10, 11, 12, 13, 14**).

Again, compounds **7**−**14** showed no depletion with increasing amounts of p38α, indicating no interaction. These results suggest again a weak interaction (K_D > 10 μM). The time required for each pairwise measurement is again 10−15 min. The sample consumption for these experiments was 25 pmol (5 μL of a 5 μM inhibitor solution) of each inhibitor and 25−75 pmol (5 μL of a 5−15 μM protein solution) of protein. Two to three measurements with increasing protein concentration were collected for each inhibitor pair to assign a relative binding affinity.

Kinetic Method. The extraordinarily slow binding kinetics of p38α with **4** and BIRB796-analogues are described in the literature.[19,21,22] While ATP competitive type I kinase inhibitors,
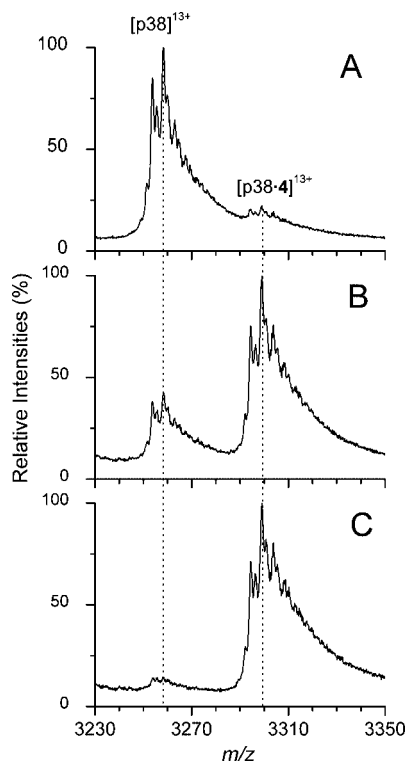
Figure 6. Determination of the real protein concentration of p38α. A representative mass spectrum of "5 μM" of p38α is shown in (A) ([p38α]^{13+}) (the total protein concentration was determined using RP-HPLC as described in the experimental section). (B, C) Representative mass spectra of "5 μM" p38α incubated with different concentrations of **4**, 0.5 μM (B) and 1 μM (C) after an incubation time of 2 h where binding equilibrium is assumed. At a ligand concentration of 1 μM (C) a shift of the intensity to [p38α·**4**]^{13+} is observed, indicating that p38α is almost fully complexed with **4**. This implies that the free "5 μM" p38α concentration is actually closer to 1 μM, since 85−90% of p38α is complexed at this concentration (determined by integration of the peak areas).

for example, compound **2** for the p38α target, have typical k_{on} rates of 1.5×10^7 M^{-1} s^{-1} and k_{off} rates of 1.8×10^{-1} s^{-1},[19] type II kinase inhibitors like **4** can have k_{on} rates of 8.49×10^4 M^{-1} s^{-1} and k_{off} rates of 8.3×10^{-6} s^{-1}. In other words, the half life calculated for the dissociation of **4** from p38α is 23 h.[21] Two ligands of our list showed binding kinetics slow enough to be followed by our instrumentation (**4**, **17**), even though other ligands in Table 1 are reported to have relatively slow k_{on} and k_{off} rates (**15**, **16**, **17** as described in literature).[31] The problem here is that the dead time before a measurement is approximately 1 min (time needed for mixing the solutions, for the NanoMate to pick up a pipet, fill it, get into spray position, start, and stabilize the spray with the voltage turned on).

As described in the experimental section, it is important use an excess of [L]$_0$ over [p38α]$_0$ for the first order approximation to hold. To estimate the real protein concentration of our p38α sample, we incubated p38α with different concentrations of **4** and collected mass spectra after 2 h, at which point equilibrium should be established. At the concentrations used, p38α should be fully (>97%) complexed with **4** based on this inhibitor's very low K_D, 3.4 nM.[9] Figure 6 shows representative mass spectra of a "5 μM" (A) solution of
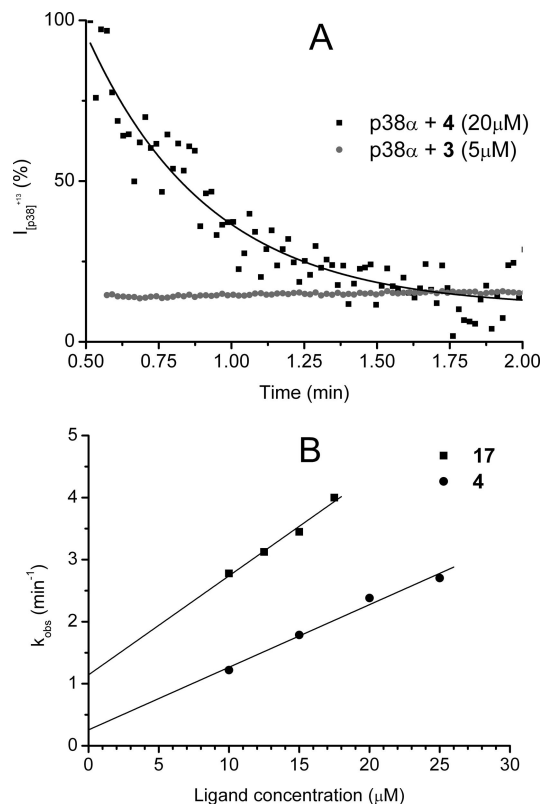
Figure 7. (A) Time traces of p38α and noncovalent p38α-ligand complexes for inhibitors with different interaction types. One micromolar p38α incubated with **3** (5 μM) shows that binding equilibrium is reached <0.5 min after mixing, corresponding to fast, competitive binding kinetics. However, 1 μM p38α incubated with **4** (20 μM) shows that binding equilibrium is only reached after approximately 2 min, corresponding to a very low k_{on} rate for the complexation. From the slope the k_{obs} can be determined as described in the Experimental Section and Methods sections. (B) Results from kinetic experiments for p38α binding **4** and **17**, respectively, at different concentrations. The obtained k_{obs} is plotted as function of the initial ligand concentration allowing the determination of k_{on}, k_{off}, and K_D.

p38α alone (total protein concentration determined using RP-HPLC, see Experimental Section), with 0.5 μM of **4** (B) and 1 μM of **4** (C) added. Since an almost complete shift (85−90%) to the [p38α·**4**]^{13+} complex is observed at a ligand concentration of 1 μM, the real p38α concentration must also be close to 1 μM, lower than the original concentration of this solution ("5 μM"). This discrepancy is most likely due to the protein desalting step applied before MS analysis, which thus must have a rather low recovery (≈20%). All experiments described in the following were performed using "5 μM" of p38α with an actual concentration of ≈1 μM.

Figure 7A shows a normalized time trace of a kinetic experiment using ≈1 μM of p38α with 7.5 μM of **4** in nondenaturing buffer. The percentage of remaining p38α ([p38α]$_t$) is plotted on the y-axis; it was determined by calculating the ratio $100 \times$ [p38α]^{13+}/([p38α]^{13+}+ [p38α·L]^{13+}) using peak intensities of the corresponding signals as a function of time.

Further kinetic experiments were performed by using five different concentrations of ligand in excess compared to ≈1 μM p38α. The individual k_{obs} were determined as described

Table 2. Comparison of Our IC₅₀ Data and Available Literature to Results for p38α for the Noncovalent Complex Competition Method and the Ligand Depletion Method[a]

A						
compound	**3**	**2**	**16**	**5**	**15**	**14**
IC$_{50}$ (μM)	0.035	0.031	0.088	0.86	2.597	7.566
ref 9; K_Ds (μM)	0.0032	0.013		0.26		

B						
noncovalent complex competition method	**3** (K_D = 34 nM)	**2**	**16**	**5**	**15**	**14**
ligand depletion method	**3** (K_D = 4.7 nM)	**2**	**16**	**5**	**15**	**14**

[a] Table 2A lists all IC$_{50}$ values determined for compounds **3**, **2**, **5**, **14**, **15**, and **16**, and Table 2B shows the affinity order (decreasing affinity from left to right) determined by our MS methods. The K_D values determined by the noncovalent titration method and the titration method in the low mass range are given in parenthesis for compound **3**.

in the Experimental Section). By plotting the k_{obs} against the ligand concentration (Figure 7B), k_{on} and k_{off} can be determined by the slope and the intercept, respectively, see eq 3. The K_D value can be determined by eq 2.

As shown below (Table 3), a k_{on} of $(1.7 \pm 0.1) \times 10^3$ M^{-1} s^{-1}, and a k_{off} of $(3.5 \pm 1.6) \times 10^{-3}$ s^{-1} was found, corresponding to a K_D of 2.1 μM for compound **4**. For compound **17**, a k_{on} of $(2.8 \pm 0.17) \times 10^3$ M^{-1} s^{-1}, and a k_{off} of $(1.7 \pm 0.2) \times 10^{-3}$ s^{-1} was determined, corresponding to a K_D of 6.1 μM. The time consumption for five data points (to fit for k_{on}, k_{off} and K_D) for one ligand is roughly 4 h. Sample consumption for this method was 25 pmol (5 μL of the "5 μM" protein solution) of protein per data point and varying concentrations for the ligands (see x-axis of Figure 7B). The IC$_{50}$ values obtained were 0.012 μM and 0.086 μM for **4** and **17**, respectively. These values will be discussed below, in the section on the comparison of our results and with literature data for type II inhibitors.

LCK. The specificity of LCK forming noncovalent complexes observed with MS was tested in the same manner as for p38α. As negative control, LCK was mixed under nondenaturing conditions with **1** (a nonbinder for LCK, confirmed by our IC$_{50}$ measurements) showing no complexation of the protein. We therefore conclude that the noncovalent complexes detected for the inhibitors are specific.

Figure 8 shows LCK sprayed under denaturing (A) and nondenaturing conditions using two different settings for the collision energy, 17 V (B) and 25 V (C). The higher collision energy provides not only a better desolvation and better collisional cooling of the protein ions but also results in a shift in the charge states distribution from higher to lower charge. This latter effect is due to a reduced transmission through the collision cell of more highly charged ions as they experience a higher kinetic energy upon higher acceleration. However, the higher collision energy setting also destabilizes the noncovalent complexes between LCK and its inhibitors in the gas phase (see insets in panels B and C in Figure 8 for compound **6**). For this reason we performed CID experiments (as described for p38α) for the noncovalent complexes of LCK with some inhibitors (Figure 2B). The noncovalent complexes for LCK show quite different CID behavior, and there
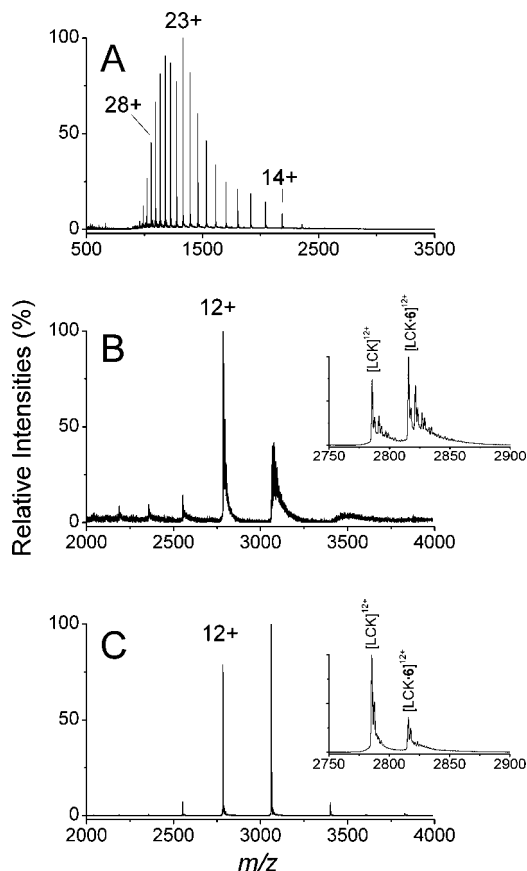

Figure 8. Representative nanoESI mass spectra of 5 μM LCK sprayed under denaturing conditions (A), and under nondenaturing conditions using 20 mM ammonium bicarbonate with two different collision energy settings: (B) 17 V and (C) 25 V. The insets in panels B and C show a zoom to charge state 12+ and the noncovalent complexes of 5 μM LCK incubated with 20 μM of **6**, observed at the collision energy settings of 17 and 25 V, respectively.

appears to be no relation to their binding affinities in solution. This is in fact more often the case. For example, in the work of Rogniaux et al. for the example of aldose reductase with inhibitors, no correlation between mass spectrometric CID experiments and IC$_{50}$ measurements performed in solution was found.[32] It is also noteworthy that the stability of the different complexes is quite different. As shown in Figure 2B, some ligand-protein complexes are very stable in the gas phase (e.g., compounds **5** and **7**) and are still 100% intact at a collision energy parameter setting of 17 V, while others are partially dissociated at this setting (e.g., compounds **6**, **8**, and **9**). Such discrepancies could arise because the number of hydrogen bonds differs for the different compounds (the small molecule ligands do have quite different structures) because of steric effects, rigidity, or number of heteroatoms (cf. Table 1). As indicated in Figure 2B, the increase of the collision energy parameter needed to achieve 50% dissociation from 18 V for compounds **6**, **8**, **9** to 22 V (for **2**, **12**) to 25 V (for **7**) to 28 V (for **5**) could indicate an increasing number of hydrogen bonds present between the ligand and the binding pocket of the protein. Unfortunately, crystal structures are not available for all the

(32) Rogniaux, H.; Van Dorsselaer, A.; Barth, P.; Biellmann, J. F.; Barbanton, J.; van Zandt, M.; Chevrier, B.; Howard, E.; Mitschler, A.; Potier, N.; Urzhumtseva, L.; Moras, D.; Podjarny, A. *J. Am. Soc. Mass Spectrom.* **1999**, *10*, 635–647.

compounds binding to LCK to support this hypothesis. These discrepancies in gas-phase stability were taken into account when ranking the affinities ranking by the noncovalent complex competition method (described in more detail later in this section).

The noncovalent complexes of LCK with compounds **2**, **6**, **8**, **9**, and **12** are almost completely dissociated at a collision energy setting of 25 V, only about 50% of the [LCK·**7**]$^{12+}$ complexes are dissociated, whereas the [LCK·**5**]$^{12+}$ complex is still >90% intact. To apply the noncovalent complex competition method to classify the LCK binding compounds by affinity, a setting of 17 V was chosen for the collision energy. This is of course a problematic compromise since at this setting desolvation of LCK ions is incomplete, as shown in Figure 8B,C. Atmosphere-vacuum interface conditions need to be as gentle as possible to maintain intact noncovalent complexes in the gas phase. Sufficient energy, however, needs to be applied to favor desolvation of the solvent shell for sensitive detection.[34] The same RF1 lens and CID settings were used for every inhibitor to be able to compare the results obtained by the noncovalent complex competition method.

The K_D of **5** binding to LCK was determined using the titration method; the value found was $5 \pm 1.5~\mu M$.

Noncovalent Complex Competition Method. In the same way as described for p38α, the small molecule inhibitors were examined in competition experiments two by two. The CID experiments performed for LCK showed a very different behavior for the different inhibitors (cf. Figure 2B). Compounds **2**, **7**, **12**, and especially **5** seem to have a higher complex stability in the gas phase compared to the rest of the compounds. To correct for this individual stability, a response factor was introduced that takes into account the percentage of intact noncovalent complex at a collision energy setting of 17 V. The response factors determined were 0.74 for compounds **2** and **12** and 0.65 for **7** and **5**. Taking into account these response factors, the following affinity order was found using the noncovalent complex competition method: **11** > **4** > **9** > **12** > **10** > **2** > **6** > **5** > **7** > **8** > **3** ≫ (**13**, **14**, **15**, **16**, **17**).

No noncovalent complexes could be detected for compounds **13**–**17**. This suggests weak to no binding to LCK ($K_D > 10~\mu M$).

Ligand Depletion Method. As described for p38α, compounds were also put into an affinity order using the ligand depletion method. It should be mentioned that some compounds (especially **5**) have considerably different ionization efficiencies compared to others (i.e., **8**, **7**) and therefore could not easily be assessed using this method. The affinity order obtained using this method was (**5**) > **10** ≈ **11** > **9** > **12** > **7** > **4** > **3** > **2** ≫ (**6**, **8**, **13**, **14**, **15**, **16**, **17**) where for the last eight compounds no or very low affinity was found because of no notable change in the intensity ratio when the LCK concentration was increased (K_D >10 μM). The differences in the affinity ranking of ligands using the noncovalent complex competition method and the ligand depletion method will be addressed in the Discussion section.

DISCUSSION

Comparing the Competitive MS Methods. The competition method where the noncovalent complexes are observed has some

(33) Yin, S.; Xie, Y.; Loo, J. A. *J. Am. Soc. Mass Spectrom.* **2008**, *19*, 1199–1208.
(34) Loo, J. A. *Mass Spectrom. Rev.* **1997**, *16*, 1–23.

Table 3. Comparison of Our Quantitative Results of the Kinetic Method, the IC_{50}, and Literature Values

compound	**4** (this paper)	**4** (ref 31)	**17** (this paper)	**4** (ref 31)
k_{on} (M^{-1} s^{-1})	1700 ± 10	8.49×10^4	2800 ± 170	1.13×10^5
k_{off} (s^{-1})	$(3.5 \pm 1.6) \times 10^{-3}$	8.3×10^{-6}	$(1.7 \pm 0.2) \times 10^{-2}$	1.4×10^{-4}
K_D (M)	2.1×10^{-6}	9.8×10^{-11}	6.1×10^{-6}	1.1×10^{-9}
IC_{50} (M)	1.2×10^{-8}		8.6×10^{-7}	

advantages over the ligand depletion method. Direct information on the noncovalent complexation (stoichiometry) of the ligand binding is obtained. Disadvantages include the relatively harsh instrumental conditions needed to detect noncovalent complexes with enough resolution, but without dissociating them. As shown for the noncovalent complexes of LCK, the setting for the collision energy is a compromise between sufficient desolvation and dissociation of the noncovalent complexes (see Figures 2B and 8). Also, the signal overlap of noncovalent complexes with ligands of similar molecular weight can render data interpretation difficult or impossible, especially when dealing with different isoforms, tagged or post-translationally modified proteins (see Figure 4).

Better sensitivity and resolution for the low m/z range of mass spectrometers are advantages of the ligand depletion method. Thus, it is no problem to distinguish two inhibitors close in molecular weight, that is, compounds **9**−**11**. A disadvantage is that the different physicochemical properties of the compounds lead to different ionization efficiencies. For example, the very high ionization efficiency of compound **5** made it impossible to assess its relative binding affinity compared to other inhibitors. This limitation was also the reason for applying this method to only two compounds at a time and for establishing a binding affinity order in a pairwise fashion.

Time (10−15 min per pair) and sample consumption (25−250 pmol per experiment) for these two methods are comparable. The advantage of the noncovalent complex competition method is that protein concentrations in the low μM range (usually 1−10 μM) are sufficient, although ligand concentrations of up to 50 μM are required, which can sometimes be a problem. The advantage of the newly reported ligand depletion method is that ligand concentrations can be in the low μM range (1−5 μM). This method could prove to be especially helpful for classification of small molecule inhibitors with low solubility in aqueous solutions. Nonetheless, protein concentrations higher than the total concentration of inhibitors are required for a sufficient depletion and assignment of the relative binding affinity.

Comparison of Our Results and with Literature Data for Type I Inhibitors. Compared to more standardized methods to assess binding of ligands to proteins, the advantage of the noncovalent complex competition method is that direct information on the noncovalent complex and the stoichiometry is obtained. Other methods rely on an indirect read-out for the abundance of the species, such as mobility shifts (Caliper technology), quantitative PCR, the fluorescence intensity, or radioactivity of dissociated versus bound compound.

Table 2A shows the comparison of our IC_{50} measurements and data obtained from the literature.[9] The compounds are listed in Tables 2B in decreasing affinity order from left to right as determined by the noncovalent complex competition method and the ligand depletion method.

p38α. The IC_{50}s and literature K_D values[9] are generally in good agreement for p38α (Table 2A). For compound **3**, the K_D value found in the literature is 3.2 nM[9] and the value of 4.7 nM determined using the titration method in the low mass range is in excellent agreement. On the other hand, the K_D value of 43 nM determined using the noncovalent titration method and the IC_{50} value of 35 nM are also in good agreement. However, there seems to be roughly 1 order of magnitude of difference between the K_D and IC_{50} values compared to values obtained by the ligand depletion method and to literature values. It is possible that the noncovalent titration method leads to somewhat elevated K_D values as some of the complex stability is lost with the instrumental parameters used (see Figure 2A and discussion about CID experiments for p38α in the Results section). However, despite these minor differences in quantitative assessment of the binding strengths, all methods plus literature point to the low nM range for **3** binding to p38α, both competitive MS methods give exactly the same affinity order as that obtained by IC_{50} measurements and from literature K_D values.[9]

LCK. A comparison between the IC_{50} values of Fabian et al.[9] and our measurements for LCK with inhibitors was also made. The IC_{50} and K_D values[9] for compounds **3, 5, 7, 8**, and **10** are all very close, in the 1−10 μM range; unfortunately the published values are given without error bars. Because of this, the affinity order varies a bit depending on the method used (i.e., **5** should have a lower affinity compared to **3** according to Fabian et al.). IC_{50} values for compounds **11** and **12** were below the micromolar range and determined to be 0.23−0.33 μM and 0.8−0.9 μM, respectively; no literature data is available for comparsion). Our MS experiments with the noncovalent complex competition method and the ligand depletion method were in good agreement with this and we were able to separate these two inhibitors from **3, 5, 7, 8**, and **10**, which belong to another affinity class. With the titration method described by Daniel et al.[27] we found a K_D value for **5** of 5 ± 1.5 μM binding to LCK, so we know the affinity class (low μM range) of this compound, which is the same obtained by the IC_{50} measurements and reported in the literature.

Comparison of Our Results and with Literature Data for Type II Inhibitors. According to the literature,[9,31] as well as our IC_{50} measurements, compound **4** has the highest affinity for p38α as shown in Table 3. Both our competitive MS methods revealed the same information. However, the K_D values from the literature[31] appear to be too low, in the pM range, rather than in the nM range as determined by our IC_{50} measurements, as well as our kinetic method. The latter proved to be very useful to differentiate **4** and **17** (both type II inhibitors) from type I inhibitors because the slow binding can be directly monitored by mass spectrometry (Figure 7). Moreover, as described above, this technique can be used to quantitatively measure the binding strength.

Table 3 gives a summary of our results on K_D determination for **4** and **17** and a comparison with literature values.[31] There is a difference of roughly 1 order of magnitude for the k_{on} and 3 orders of magnitude for the k_{off} rates, resulting in a K_D with around 2 orders of magnitudes of difference compared to literature values. There are also considerable differences for the values measured for **17**. The reasons for these differences are not entirely clear. The use of different solution conditions (buffer composition, pH, ionic strength, temperature), might influence the conformation and/or activity of the protein and also the binding process. Another reason for the differences may be the fact that in our work we directly measure the appearance of the noncovalent complex and disappearance of free protein signal as opposed to the method reported in the literature[31,35] where a fluorescent probe is in competition with the investigated inhibitor (indirect measurement). In this case, the kinetic constants are measured in competition with another binding probe, whereas in our case only the binding of **4** is observed directly. It is unclear whether this competing fluorescent probe could interfere with the equilibrium between the active ("DFG-in") and inactive ("DFG-out") form of p38α found in solution.[19] Distortion of this equilibrium could completely alter the binding kinetics for the association of **4** to the inactive p38α.

CONCLUSIONS

For the kinases p38α and LCK interacting with different inhibitors we could demonstrate that two different MS-based techniques can be used to determine K_D values that are in good agreement with IC_{50} values and literature data obtained in solution phase. Using the competition methods (the noncovalent complex competition method and the ligand depletion method) a series of inhibitors were successfully screened and ordered according to their relative affinity. Within 8 h of measurement per method, a series of 15 inhibitors can be put into affinity order for one protein target. This technique can present a powerful tool, if for example the K_D of a lead structure is determined (or known by other methods) and a series of compounds needs to be tested against it. The benefits of using these MS-based methods are that no labeling (of protein/substrate) is required, low sample consumption is guaranteed using the NanoMate (4 μL of a 5 μM protein solution for one data point), and direct information about stoichiometry (specificity of the binding) can be assessed.

Differentiation of type I from type II inhibitors is possible with our newly described kinetic method. This new approach also allows K_D determination by measuring k_{on} and k_{off} rates of the binding, as demonstrated for p38α and **4** and **17**.

(35) Morelock, M. M.; Pargellis, C. A.; Graham, E. T.; Lamarre, D.; Jung, G. *J. Med. Chem.* **1995**, *38*, 1751–1761.